

12-1-1996

A Stochastic Model for Crystal-amorphous Transition in Low Temperature Molecular Beam Epitaxial Si(111)

R. Venkatasubramanian
University of Nevada, Las Vegas

Suresh Gorantla
University of Nevada, Las Vegas

S. Muthuvenkatraman
University of Nevada, Las Vegas

Donald L. Dorsey
Wright Laboratory WL/MLPO

Follow this and additional works at: https://digitalscholarship.unlv.edu/ece_fac_articles



Part of the [Electronic Devices and Semiconductor Manufacturing Commons](#), [Other Electrical and Computer Engineering Commons](#), [Other Materials Science and Engineering Commons](#), and the [Semiconductor and Optical Materials Commons](#)

Repository Citation

Venkatasubramanian, R., Gorantla, S., Muthuvenkatraman, S., Dorsey, D. L. (1996). A Stochastic Model for Crystal-amorphous Transition in Low Temperature Molecular Beam Epitaxial Si(111). *Journal of Applied Physics*, 80(11), 6219-6222.

https://digitalscholarship.unlv.edu/ece_fac_articles/605

This Article is protected by copyright and/or related rights. It has been brought to you by Digital Scholarship@UNLV with permission from the rights-holder(s). You are free to use this Article in any way that is permitted by the copyright and related rights legislation that applies to your use. For other uses you need to obtain permission from the rights-holder(s) directly, unless additional rights are indicated by a Creative Commons license in the record and/or on the work itself.

This Article has been accepted for inclusion in Electrical and Computer Engineering Faculty Publications by an authorized administrator of Digital Scholarship@UNLV. For more information, please contact digitalscholarship@unlv.edu.

A stochastic model for crystalamorphous transition in low temperature molecular beam epitaxial Si (111)

R. Venkatasubramanian, S. Gorantla, S. Muthuvenkatraman, and D. L. Dorsey

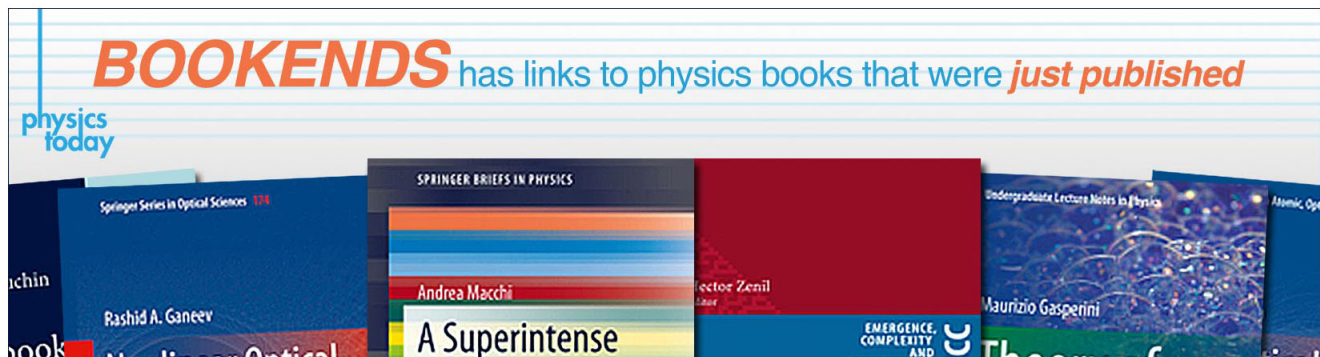
Citation: *Journal of Applied Physics* **80**, 6219 (1996); doi: 10.1063/1.363698

View online: <http://dx.doi.org/10.1063/1.363698>

View Table of Contents: <http://scitation.aip.org/content/aip/journal/jap/80/11?ver=pdfcov>

Published by the [AIP Publishing](#)

Advertisement:

An advertisement for 'BOOKENDS' featuring a banner with the text 'BOOKENDS has links to physics books that were just published'. Below the banner, several book covers are displayed, including 'Springer Series in Optical Sciences' by Rashid A. Ganeev, 'A Superintense' by Andrea Macchi, 'EMERGENCE, COMPLEXITY AND...' by Professor Zenil, and 'Undergraduate Lecture Notes in Physics' by Maurizio Gasperini. The 'physics today' logo is visible in the top left corner of the advertisement.

A stochastic model for crystal-amorphous transition in low temperature molecular beam epitaxial Si (111)

R. Venkatasubramanian,^{a)} S. Gorantla, and S. Muthuvenkatraman
*Department of Electrical and Computer Engineering, University of Nevada, Las Vegas,
Las Vegas, Nevada 89154*

D. L. Dorsey^{b)}
Materials Directorate, Wright Laboratory, WLM/MLPO, WPAFB, Ohio 45433

(Received 26 June 1996; accepted for publication 22 August 1996)

Molecular beam epitaxial Si (111) grown below a certain temperature result in amorphous structure due to the limited surface mobility of atoms in finding correct epitaxial sites. In spite of many experimental and theoretical studies, the mechanism of crystal-amorphous transition and its dynamics related to the growth conditions are not well understood. In this article, we present a theoretical model based on the formation of stacking fault like defects as a precursor to the amorphous transition of the layer. The model is simulated based on a stochastic model approach and the results are compared to that of experiments for temperatures in the range of 500–900 K and growth rate in the range of 0.1–3.0 Å/s. The agreement between our results and experimental observations is excellent. © 1996 American Institute of Physics. [S0021-8979(96)00723-2]

I. INTRODUCTION

Molecular beam epitaxy (MBE) of Si has attracted much attention in the past few years because of the simplicity of the mono-atomic epitaxial system and the possibility of new device applications. In Si MBE growth, the low temperature growth material exhibits amorphous structure due to limited surface migration. Low temperature growth of Si has been the subject of several experimental^{1–7} and theoretical^{2,3,6} studies. An excellent review of these works is presented in Ref. 3. A variety of experimental tools, scanning tunneling microscopy⁴, transmission electron microscopy,^{2,5} reflection high energy electron diffraction² and Rutherford back scattering⁶ have been used to study the low temperature epitaxy. The general conclusions of these works are: for a given growth condition, there is a fixed thickness, h_{epi} , up to which the epitaxial layer is crystalline and then turns into amorphous material; the h_{epi} is growth condition and orientation dependent; h_{epi} versus temperature dependence follows an Arrhenius type rate behavior with an activation energy of 0.45 eV for Si (100). The activation energy slightly increases with increasing growth rate. The temperature of transition to amorphous growth from crystalline growth is found to be orientation dependent with a temperature difference of about 300 K between (100) and (111) growths. It was observed that the temperature regime of amorphous-crystalline transition for Si (111) is sharp and occurs over a 150 K range.⁶

There are a few theoretical models developed and used to study the low temperature epitaxy (LTE) of Si and other materials: continuous break down model,² defect accumulation model,³ hydrogen and impurity segregation model⁸ and roughening model.³ These models explain some features of the LTE phenomenon, but not all of them. Thus there is a need to develop a model which will capture all the necessary physics and clarify all the experimental observations.

In this article, we adopt a kinetic model based on defect formation⁹ for studying the LTE phenomenon in Si (111) and describe it using a stochastic model of growth. In Sec. II, details of the proposed kinetic model and the stochastic model are presented. In Sec. III, results of the stochastic model are compared with the experimental work of Ref. 6. Conclusions are presented in Sec. IV.

II. KINETIC AND STOCHASTIC MODEL

A. The kinetic model

Note that in the case of low temperature Si [111] MBE growth, the bonding geometry allows for the easy formation of stacking faults which accumulates over many layers and ultimately leads to amorphous growth. If the thermal energy is high enough for the Si atoms at the wrong site to migrate to a correct site, then they make a correcting hop to a nearest neighbor correct site. Thus the epitaxial layer grows as crystalline. This paper has adopted such a kinetic model and developed a stochastic model to test its validity.

B. The stochastic model

The stochastic model is based on the master equation approach with random distribution approximation for the surface atomic configurations. Details of the stochastic model are presented in Ref. 9,10. The layer sequence in a diamond cubic crystal growing along [111] direction is: AaBbCc where atoms in the a, b and c layers are singly covalent bonded to the surface (secondary) and the ones in A, B and C layers are triply covalent bonded to the surface (primary). Two surface kinetic processes are considered in the model: adsorption and intralayer migration. Evaporation and interlayer migration are assumed negligible due to low temperature. The adsorption of Si atoms can occur at two different sites in a layer; the correct site and the stacking fault site. It should be noted that the occupation of an A(B) site disallows occupation of the three adjacent B(A) sites due to bond angle constraints. Similar constraints hold for C atoms too.

^{a)}Electronic mail: venkat@unlv.edu

^{b)}Electronic mail: dorseydl@wl.wpafb.af.mil

The time evolution of the epitaxial crystal can be described in terms of the rates of change of independent macro-variables of growth, (i.e.), concentration variables, $C_A(n)$, $C_B(n)$, and $C_C(n)$, and the atom-vacancy pair variables, $Q_A(n)$, $Q_B(n)$, and $Q_C(n)$. The rate of change of these macro-variables can be described in terms of the rates of adsorption and surface migration processes as described in Ref. 9,10.

For the primary layers, the adsorption rate of atoms at A type sites in the n^{th} layer, $[dC_A^{\text{ads}}(n)]/dt$, is given by

$$\frac{dC_A^{\text{ads}}(n)}{dt} = \frac{J}{3} (F_B(n-1) + F_C(n-1) - C_A(n) - W_B(n) - W_C(n)), \quad (1)$$

where J is the flux and 3 in the denominator is to allow equal flux for all three sites. $F_B(n-1)$ and $F_C(n-1)$ are the A sites created by the $n-1^{\text{th}}$ layer B and C atoms, respectively, through triple covalent bonding coordination and are given by

$$F_B(n-1) = C_B(n-1) \left(\frac{\tilde{N}_{BB}(n-1)}{3C_B(n-1)} \right)^2 \quad (2)$$

and

$$F_C(n-1) = C_C(n-1) \left(\frac{\tilde{N}_{CC}(n-1)}{3C_C(n-1)} \right)^2, \quad (3)$$

where $\tilde{N}_{BB}(n-1)$ and $\tilde{N}_{CC}(n-1)$ are the normalized (to the number of sites in the layer, N) concentrations of B atom-B atom and C atom-C atom pair configurations, respectively, in the $n-1^{\text{th}}$ layer. $F_B(n-1)$ and $F_C(n-1)$ account for the formation of triangular pairs necessary to form triple covalent bonds with subsequent layers. In the limit of $C_B(n-1)$ tending to 1, $\tilde{N}_{BB}(n-1)$ tends to $3C_B(n-1)$ and, hence, $F_B(n-1)$ tends to 1 according to Eq. 2, which is correct. In the limit of $C_B(n-1)$ tending to 0, $\tilde{N}_{BB}(n-1)$ tends to 0 and, hence, $F_B(n-1)$ tends to 0 according to Eq. 2, which is also correct.

$W_B(n)$ and $W_C(n)$ are the concentrations of A sites which are wasted due to the presence of B and C type atoms, respectively, and are given by

$$W_B(n) = C_B(n) \left(1 + \left(\frac{Q_B(n)}{6C_B(n)} \right) + \left(\frac{Q_B(n)}{6C_B(n)} \right)^2 \right) \quad (4)$$

and

$$W_C(n) = C_C(n) \left(1 + \left(\frac{Q_C(n)}{6C_C(n)} \right) + \left(\frac{Q_C(n)}{6C_C(n)} \right)^2 \right), \quad (5)$$

respectively. $Q_B(n)$ and $Q_C(n)$ are the concentrations of B atom-vacancy and C atom-vacancy pairs in the n^{th} layer. Details of the derivation are left out due to space limitations. Note that in the limit that the concentration of B atoms is small, $Q_B(n)$ tend to $6C_B(n)$ and, hence, $W_B(n)$ tends to $3C_B(n)$, i.e., every B atom wastes 3 A atoms sites, which is correct. In the limit of $C_B(n)$ tending to unity, $Q_B(n)$ is 0 and, hence, $W_B(n)$ tends to $C_B(n)$, i.e., almost all A sites are wasted, which is also correct. A schematic picture describing the above limits is shown in Figure 1. The isolated B atom in

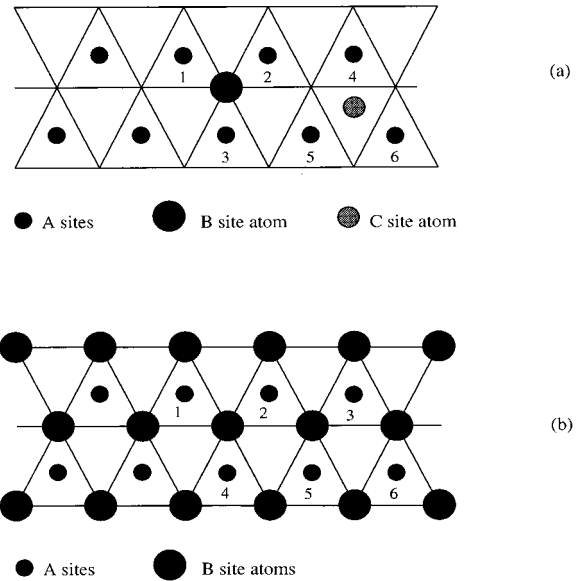


FIG. 1. A schematic picture of atomic arrangement in (111) plane depicting the wastage of one type of site due to the presence of atom at another type of site.

Figure 1 (a) prevents the occupation of three sites denoted 1, 2 and 3. When the layer is completely occupied by B atoms, all A sites (one A site for every B atom) are prevented from occupation as shown in Figure 1(b).

The rate of change of A atom-vacancy pair concentration, Q_A , due to adsorption of an A atom is given by

$$\frac{dQ_A^{\text{ads}}(n)}{dt} = \frac{J}{3} (F_B(n-1) + F_C(n-1) - C_A(n) - W_B(n) - W_C(n)) \left(\frac{\tilde{N}_{VVA}(n) - \frac{1}{2}Q_A(n)}{3C_{VA}(n)} \right) \quad (6)$$

for primary layers, where $\tilde{N}_{VVA}(n)$ and C_{VA} are the normalized vacancy-vacancy pair and vacancy concentrations, respectively for the A site.

Intralayer migration of atoms is allowed from the wrong sites to the correct sites. If the wrong sites in a layer are B and C, then atoms at B and C can migrate to an A site. All other types of migrations are expected to be negligible due to low thermal activation compared to the bond energies. We call this type of migration the correcting hop process. The correcting hop process will result in better crystallinity of the epitaxial layer. The rate of migration of a wrong site atom (say B) to a correct site (say A) in the n^{th} layer based on Arrhenius type rate behavior, is given by

$$\frac{dC_A^{\text{mig}}(n)}{dt} = 6 \times R_{\text{iso}}^{\text{mig}} \left(\frac{C_B(n)}{C(n)} \right) (C(n) - C(n+1)) \times (F_B(n-1) + F_C(n-1) - C_A(n) - W_B(n) - W_C(n)) \times \left(\frac{\tilde{N}_{AA}(n) e^{-K_A} - \frac{1}{2}Q_A(n) e^{K_A}}{3C_A(n)} \right)^6 \quad (7)$$

for the primary layers, where R_{iso}^{mig} is the migration rate of an isolated B atom, $\{[C_B(n)]/[C(n)]\}[C(n) - C(n+1)]$ is the fraction of B site atoms available for migration and $\{[\tilde{N}_{AA}(n)e^{-K_A} - \frac{1}{2}Q_A(n)e^{K_A}]/[3C_A(n)]\}^6$ is the energy term accounting for the nearest neighbor binding within the layer. The number 6 in Eq. 7 is the inplane co-ordination number and $K_{AA} = V_{AA}/(k_B T)$ is the normalized energy parameter with V_{AA} the atom pair binding energy, k_B the Boltzmann constant and T the temperature in K.

The rate of change of A atom-vacancy pair concentration, $Q_A(n)$, due to migration of a B atom into an A site, is given by

$$\begin{aligned} \frac{dQ_A^{mig}(n)}{dt} &= 6 \times R_{iso}^{mig} \left(\frac{C_B(n)}{C(n)} \right) (C(n) - C(n+1)) \\ &\quad \times (F_B(n-1) + F_C(n-1) - C_A(n) \\ &\quad - W_B(n) - W_C(n)) \\ &\quad \times \left(\frac{\tilde{N}_{AA}(n)e^{-K_A} + \frac{1}{2}Q_A(n)e^{K_A}}{3C_A(n)} \right)^6 \\ &\quad \times \left(\frac{\tilde{N}_{VVA}(n) - \frac{1}{2}Q_A(n)}{3C_{VA}(n)} \right) \end{aligned} \quad (8)$$

for the primary layers. The rate of change of B atom-vacancy pair concentration, $Q_B(n)$, due to migration of a B atom into an A site, is given by

$$\begin{aligned} \frac{dQ_B^{mig}(n)}{dt} &= 6 \times R_{iso}^{mig} \left(\frac{C_B(n)}{C(n)} \right) (C(n) - C(n+1)) \\ &\quad \times (F_B(n-1) + F_C(n-1) - C_A(n) \\ &\quad - W_B(n) - W_C(n)) \\ &\quad \times \left(\frac{\tilde{N}_{AA}(n)e^{-K_A} + \frac{1}{2}Q_A(n)e^{K_A}}{3C_A(n)} \right)^6 \\ &\quad \times \left(\frac{\tilde{N}_{AA}(n)e^{-K_A} - \frac{1}{2}Q_A(n)e^{K_A}}{\tilde{N}_{AA}(n)e^{-K_A} + \frac{1}{2}Q_A(n)e^{K_A}} \right) \end{aligned} \quad (9)$$

for the primary layers. Expressions for the secondary layers can be obtained by replacing $[F_B(n-1) + F_C(n-1) - C_A(n) - W_B(n) - W_C(n)]$ with $[C_A(n-1) - C_A(n)]$ in Eqs. 1,6-9 due to change in the subsurface covalent bonds from 3 to 1.

The total rate of time variation of $C_A(n)$ and $Q_A(n)$ is given by

$$\frac{dC_A(n)}{dt} = \frac{dC_A^{ads}(n)}{dt} + \frac{dC_A^{mig,in}(n)}{dt} - \frac{dC_A^{mig,out}(n)}{dt} \quad (10)$$

and

$$\frac{dQ_A(n)}{dt} = \frac{dQ_A^{ads}(n)}{dt} + \frac{dQ_A^{mig,in}(n)}{dt} - \frac{dQ_A^{mig,out}(n)}{dt}, \quad (11)$$

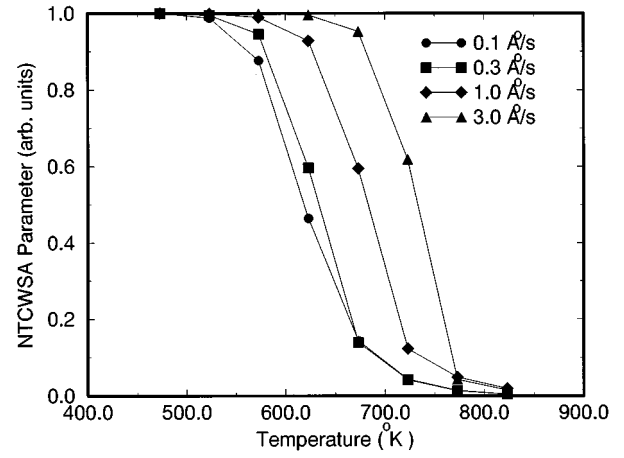


FIG. 2. Plots of normalized time averaged concentration of wrong site atoms parameter versus growth temperature for various growth rates.

respectively, where the terms ‘in’ and ‘out’ in the superscript refer to atoms migrating into and out of the A site.

Expressions similar to Eqs. 10 - 11 can be written for B and C atoms for the n^{th} layer. Thus, there are six time evolution equations per layer which are coupled, nonlinear, first order differential equations and are not analytically integrable. These equations for 24 consecutive layers (maximum considered due to computational limitations) were solved using numerical integration on a SUN Sparc station. The CPU time for a typical growth simulation of 10 s was about 1 CPU hour.

III. RESULTS AND DISCUSSION

Due to the lack of published values for model parameters, such as the activation energy for intralayer migration and second nearest neighbor atom pair interaction energy for the Si MBE growth system, the following values were chosen. The atom pair interaction energies were assumed to be: $V_{A-A} = V_{B-B} = V_{C-C} = 0.2$ eV. The frequency factor for intralayer migration is assumed to be 2×10^{11} /s. The activation energy for intralayer migration of an isolated wrong site atom is assumed to be 1.3 eV, which is a typical value measured and used for several semiconductors. The substrate temperature was chosen in the range (400–900 K) and the growth rate was in the range 0.1–3 Å/s.

By numerical integration, the solution to the differential equations was obtained. From the concentration variables, $C_A(n)$, $C_B(n)$, and $C_C(n)$, using the following expression, the normalized time averaged concentration of wrong site atoms, $NTCWSA$, was obtained as

$$NTCWSA = \frac{\int_0^T \sum_{i=1}^{i=20} \left(\frac{TWSA - TNA}{TNA} \right) dt}{T}, \quad (12)$$

where $TWSA$ and TNA are the total number of wrong site atoms and total number of atoms, respectively and T is the total time of growth, which was 10 s for all our growth simulations.

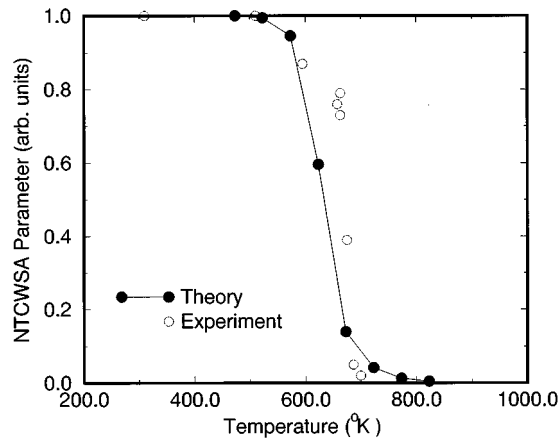


FIG. 3. Plots of normalized time averaged concentration of wrong site atoms parameter versus growth temperatures for 0.3 Å/s along with experimental data of Weir *et al.*⁶

The *NTCWSA* was obtained for various growth temperatures and growth rates. Plots of *NTCWSA* versus growth temperature are shown in Figure 2 for growth rates in the range 0.1–3 Å/s. It is observed that the *NTCWSA* parameter decreases with increasing temperature and becomes very small at high temperatures, indicating growth of good crystalline quality material with less stacking faults, which is in agreement with the experimental observations of Weir *et al.*⁶ At low temperature, the layers are completely randomly filled indicating a high degree of stacking faults which according to our model represents an amorphous material. The *NTCWSA* versus temperature plot is shown along with experimental data of Weir *et al.*⁶ in Figure 3, and the agreement between the results is excellent. The temperature range of transition is 100–200 K which compares well with Weir *et al.*,⁶ for 0.3 Å/s as shown in Figure 3. Additionally, the transition itself moves towards lower temperatures for lower growth rates as shown in Figure 2, which is consistent with increased effective migration rate of atoms at lower growth rate and high temperatures.

A plot of half temperatures of transition, $T_{1/2}$ (at which half of the layers are amorphous, i.e., $NTCWSA = 0.5$), is shown as a function of growth rate along with the experimental data of Weir *et al.*⁶ in Figure 4. Qualitatively, results of the theory and experiments exhibit the same trend: the $T_{1/2}$ increases with increasing growth rate. Quantitatively the agreement is within about 50 K. Better agreement can be achieved by careful choice of parameters such as activation energies and frequency factors.

Due to the computational time limitations, we did not attempt to study the thickness limited epitaxy issue. But the general trends observed in the thickness limited epitaxy experiments are observed in our results: epitaxial thickness is larger for higher temperatures and lower growth rates, which is consistent with increased effective rates of correcting hops observed in our results.

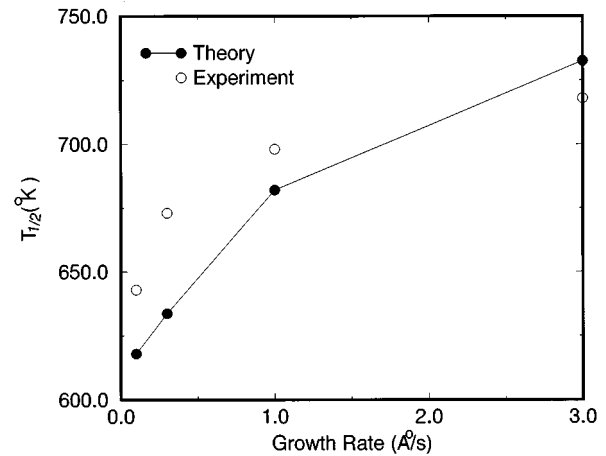


FIG. 4. Plot of $T_{1/2}$ versus growth rate with experimental data.⁶

The model is general and can be adopted for other orientational growths and other material systems. The limitations of the model are that it only simulates amorphous structure indirectly through stacking faults and, due to computational time limitations, we cannot study thickness limited epitaxy.

IV. CONCLUSION

We have developed a theoretical model for studying the crystal-amorphous transition in MBE grown Si (111) model based on the formation of stacking faults as a precursor to amorphous transition of the layer. The model is simulated based on a stochastic model approach and the results are compared to experiments. The agreement between our results and experimental observations is excellent for various growth conditions. The model is general and can be modified for studying other material systems and orientations.

ACKNOWLEDGMENT

The initial work was performed at the US Air Force Wright Laboratory, WL/MLPO, WPAFB, Dayton, Ohio, as part of a summer faculty fellowship program during summer 1992.

- ¹M. Ichikawa, *Mater. Sci. Eng. R. Rep.* **4**, 147 (1986).
- ²H. Jorke, H. J. Herzog, and H. Kibbel, *Phys. Rev. B* **40**, 2005 (1989).
- ³D. J. Eaglesham, *J. Appl. Phys.* **77**, 3597 (1995).
- ⁴Y.-W. Mo, R. Kariotis, B. S. Swartzneruber, M. B. Webb, and M. G. Legally, *J. Vac. Sci. Technol. B* **1**, 808 (1983).
- ⁵D. J. Eaglesham, H.-J. Gossman, and M. Cerullo, *Phys. Rev. Lett.* **65**, 1227 (1990).
- ⁶B. E. Weir, B. S. Freer, R. L. Headrick, D. J. Eaglesham, G. H. Gilmer, J. Bevk, and L. C. Feldman, *Appl. Phys. Lett.* **59**, 204 (1991).
- ⁷M. V. Ramana Murty and H. A. Atwater, *Phys. Rev. B* **49**, 8483 (1994).
- ⁸D. J. Eaglesham, F. C. Unterwald, H. Luftman, D. P. Adams, and S. M. Yalisove, *J. Appl. Phys.* **74**, 6615 (1993).
- ⁹R. Venkatasubramanian, *J. Mater. Res.* **7**, 1222 (1992).
- ¹⁰R. Venkatasubramanian, *J. Mater. Res.* **7**, 1236 (1992).